PERFORMANCE OF AN ACTIVE VIBRATION ISOLATION SYSTEM

Ryuhei Sugahara, Mika Masuzawa and Hiroshi Yamaoka
High Energy Accelerator Research Organization (KEK), Tsukuba, Ibaraki, Japan

1. INTRODUCTION

In the future linear collider project, the tunnel floor stability is required to be several tens of nanometers in the main linac section, and sub-nanometer in the interaction region in the vertical direction [1]. These severe tolerances are required in order to transport and collide very small beams. The beam size is several nanometers vertically, and several hundred nanometers horizontally at the interaction point. In order to achieve this stability, some vibration isolation system will be needed. Active vibration system utilizing piezoelectric actuators were tested and their performance was reported [2-4]. An active vibration isolation system, utilizing pneumatic valves, was fabricated and tested. Test results on performance of this active vibration isolation system are reported.

2. ACTIVE VIBRATION ISOLATION SYSTEM

2.1. Hardware

An active vibration isolation system was fabricated by Tokkyokiki Corporation. Area of the table is 1200×1200 mm^2 and the height is 497 mm when the air spring is active. Weight is 1100 kg for the table and 170 kg for the base part. Bearable weight is 500 kg. The active vibration isolation is achieved by eight pneumatic control valves, two valves for X position control, two for Y and four for Z (vertical position). Pressure of the output air from a compressor is 0.6 MPa, which is lowered to 0.3 MPa by regulators. This 0.3 MPa air is supplied to the pneumatic control valves. These eight pneumatic valves are capable of not only the movement in three directions but also the rotation around each axis. Rotation angles around X, Y and Z-axis are called θ_x, θ_y and θ_z, respectively. Schematic drawing for the layout of the pneumatic actuators and sensors are shown in Fig.1. There

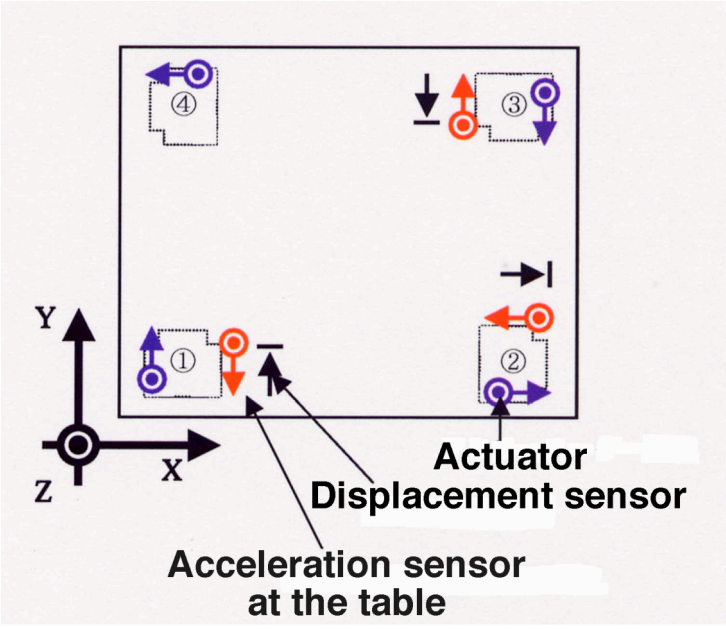

Fig. 1 Schematic drawing for the layout of actuators and sensors

are four pillars, each of which has two actuators, one for horizontal movement and another for vertical movement. At each position of three pillars, 1 to 3, two displacement sensors are set to measure relative displacement between the base and table, and two acceleration sensors are set onto the floating table. Measurement direction is shown in Fig.1. Besides these sensors, additional three acceleration sensors are attached on the base to measure acceleration of the base in three directions. Resolution of acceleration sensors is 0.1 mGal, and that of displacement sensors is 5 μm. Sensitive range of the acceleration sensor is 0.1 - 200Hz. Controller has an ADC of 16 bits and the data-sampling rate is 8kHz.

2.2. Control system

Utilizing those pneumatic actuators and sensors described in the previous section, various control scheme is possible. Table 1 shows the parameter-setting table. There are ten

Table 1: Parameter-setting table

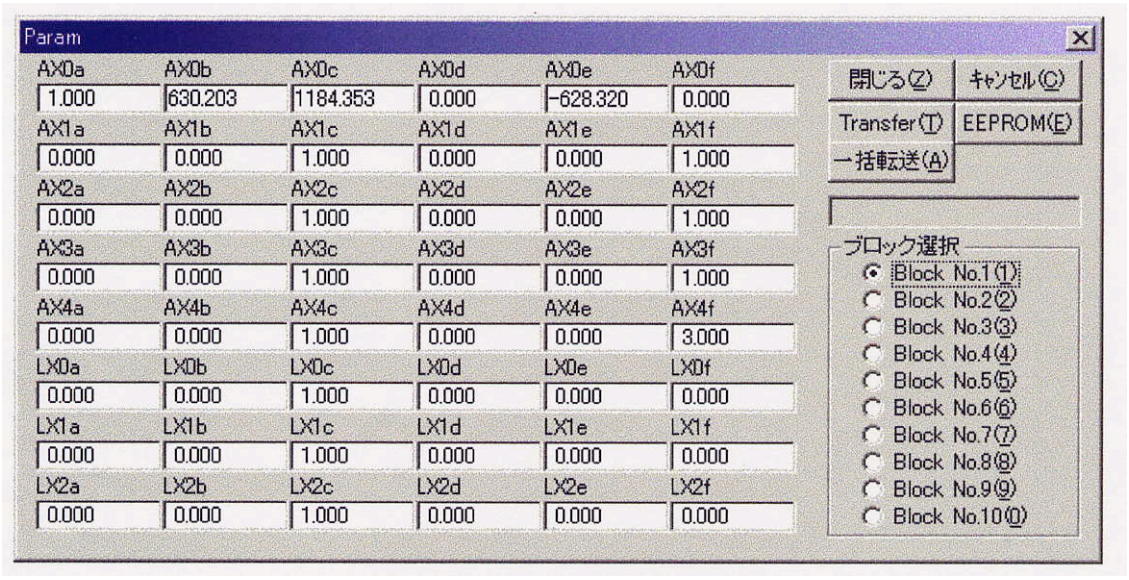

tables, which are called Block No.1, Block No.2, and so on. Function of these tables is listed in Table 2. We can set five transfer functions, G1 to G5 (row 1 to 5), for acceleration feedback control utilizing acceleration sensors at the table. And there are three transfer functions (row 6 to 8) for linear feedback control utilizing linear actuators, which are not used in our case. The transfer function has a second order form as shown in formula (1), where S stands for the variable in Laplace transform. Six columns in the table corresponds to the coefficients, a, b, c, d, e and f in the formula (1). Total transfer function G(S) is a multiplication of G1 to G5.

$$G(S) = \frac{dS^2 + eS + f}{aS^2 + bS + c} \tag{1}$$

$$G(S) = G1(S) \times G2(S) \times G3(S) \times G4(S) \times G5(S) \tag{2}$$

In this way, we can set various filters to some of G1 to G5. Actual example of eliminating resonance structure by setting a filter is shown in the following section. Parameters c and d in Block No.10 are the proportional gain and integrated mode gain for displacement control. The first row, c1 and d1, is for vertical displacement and the second row, c2 and d2, for horizontal displacement.

Table 2: Function of parameter-setting tables

Block No.1	Feedback for the table acceleration in X-direction
Block No.2	Feedback for the table acceleration in Y-direction
Block No.3	Feedback for the table acceleration in Z-direction
Block No.4	Feedback for the table acceleration in θ_x-direction
Block No.5	Feedback for the table acceleration in θ_y-direction
Block No.6	Feedback for the table acceleration in θ_z-direction
Block No.7	Feedforward with X acceleration sensor on the base
Block No.8	Feedforward with Y acceleration sensor on the base
Block No.9	Feedforward with Z acceleration sensor on the base
Block No.10	Target values for relative position and gains for displacement control

3. EXAMPLES OF SYSTEM CONTROL

3.1. Elimination of resonance

Fig.2 shows the Bode diagram of the θ_x loop transfer function for the active mode

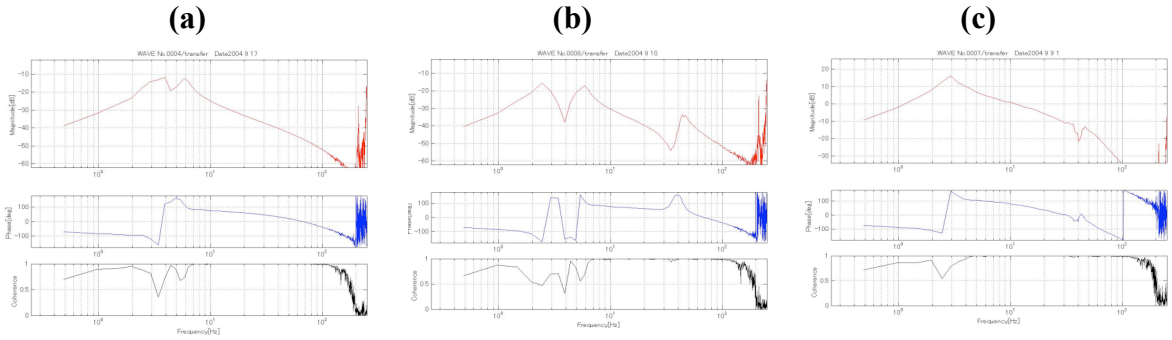

Fig. 2 Bode diagram of the θ_x loop transfer function for the active mode before parameter adjustment (a) with no load and (b) with a quadrupole magnet on the table. (c) is that after adjusting parameters.

before parameter adjustment (Par01) (a) with no load placed on the table, and (b) with a quadrupole magnet on the table. The weight of the magnet is 400 kg. Fig.2 (c) shows the same Bode diagram after parameters are adjusted (Par03). Fig.3 shows the picture of the setup when a skew-quadrupole magnet is placed on the table. A resonance structure, occurred by placing the magnet on the table, can be seen at about 40Hz in Fig.1 (b). This structure is almost eliminated as shown in Fig.1 (c) after parameters are adjusted introducing a TMD (Tuned Mass Dumper) filter.

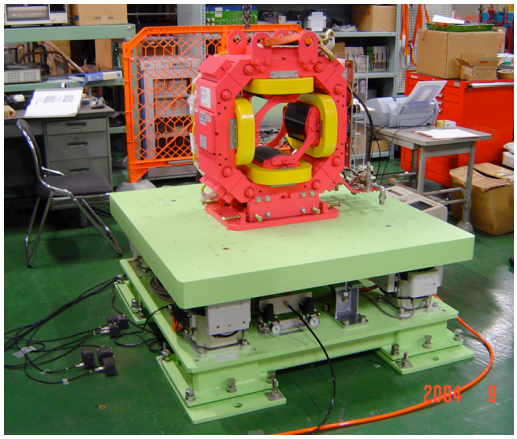

Fig. 3 A skew-quadrupole magnet is placed on the vibration isolation table. Weight of the magnet is 400 kg.

3.2. Effect of displacement conrol gain to feedback control

The controller has a capability of displacement control utilizing the displacement sensors. This feedforward displacement control can eliminate fluctuation of displacement. Fig.4 (a) shows the displacement fluctuation by about 150 μm P-P in vertical direction and about 40 μm P-P in horizontal direction. It is found that this fluctuation is caused by the

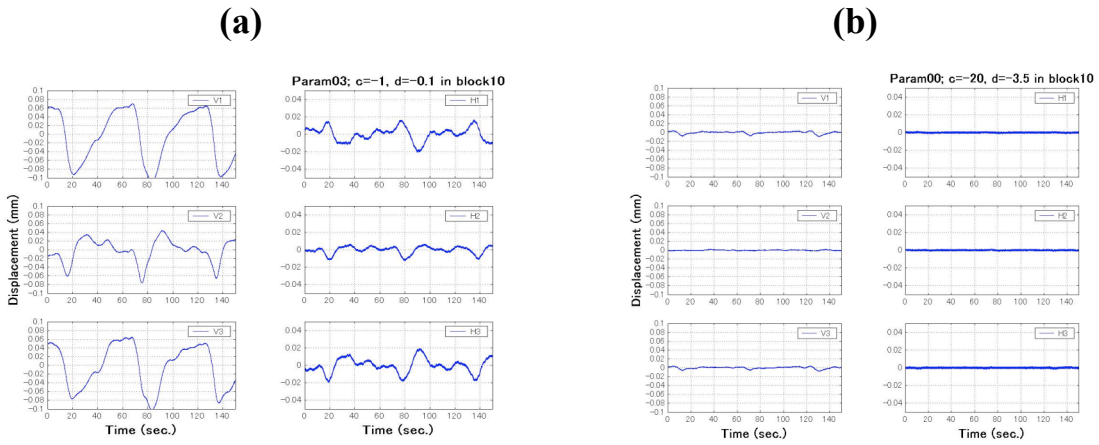

Fig. 4 Variation of displacement (a) for small displacement feed forward gains (c= -1 and d=-0.1) and (b) for big gains (c=-20 and d=-10). V1 to V3 show output from three horizontal displacement sensors and H1 to H3 output from three vertical ones.

fluctuation of the air pressure. The compressor pressurises the air up to 0.8 MPa, then stops operation until the air pressure drops to 0.6 MPa. This air is fed to regulators, and the pressure is controlled at 0.3 MPa. But the output air from regulators has the pressure fluctuation by 6 kPa because of the pressure control precision of 2%. And this air fluctuation causes the fluctuation of displacement. This fluctuation can be eliminated by raising the displacement

control gains as shown in Fig.4 (b). But performance of acceleration feedback degrades when the displacement control gains are raised. This phenomenon is shown in Fig.5. The PSD ratio of movement of the table to that of the floor is shown in Fig.5 (a) for small displacement control gains and that for big displacement control gains in Fig.5 (b). When the displacement control gains are raised, it can be seen that the damping factor of the vibration degrades by about a factor of ten in PSD in the frequency region 2 to 10Hz. Movement in the frequency region higher than 10Hz is not affected. So, we should not depend on the displacement control to eliminate the displacement fluctuation, but we should solve the problem in the different way. We will adopt high precision air regulators, which have a capability of making the fluctuation of the air pressure 1/5 of the current fluctuation.

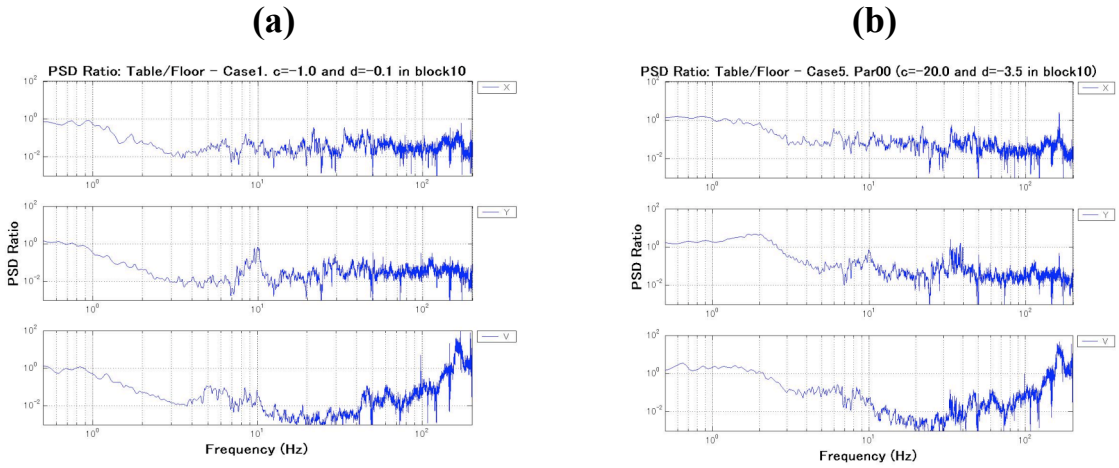

Fig. 5 PSD ratio of movement of the table to that of the floor (a) for small feedforward gains (c=-1 and d=-0.1) and (b) for big feedforward gains (c=-20 and d=-10).

4. RESULTS OF PERFORMANCE TEST

The vibration is measured on the table and on the floor in the same time with six acceleration sensors to see how much the vibration is reduced by the air spring and by the active isolation control. The sensors used in this measurement are MG-102S acceleration sensors with OSP-06 receiver of Tokkyokiki Corporation. This system has a resolution 0.1 mGal (1 μm/sec^2) and a frequency range 0.1 - 400Hz. Output unit is 1 V/Gal. Signals are measured and recorded with the data logger, Graduo DS2000 series of Onosokki Co. Ltd. Input signals are measured with 24 bit ADC.

PSD (Power Spectrum Density) of the vibration is shown in Fig.6. Firstly, the vibration is measured without air spring (Case1), then the air spring is turned on (Case3), and finally the active isolation control is turned on (Case4). In each figure, top spectrum is the PSD for X movement, middle for Y, and bottom for Z, respectively. The first figure shows the spectrum for the movement of the floor, and the rest figures show those of the table. With the air spring, it can be seen that the vibration is reduced in the frequency region higher than 10Hz but the resonant vibration at 3 and 5Hz is enhanced. By turning on the active isolation control, these 3 and 5Hz peaks are eliminated. Damping of vibration with air spring and active isolation control can bee seen clearly in Fig.7, which shows the PSD ratio of the movement of the table

to that of the floor. In Fig.7, (a) is the PSD ratio without air spring (Case1), (b) that with air spring (Case3) and (c) that with active isolation control (Case4). The damping factor is about two orders of magnitude in PSD with air spring in the frequency region higher than 10Hz. And the vibration in the low frequency region is reduced with the active isolation control. The damping factor is about one to two orders of magnitude in the frequency region 2 - 100Hz. We install a band pass filter to damp the vibration only in the frequency region 0.01 - 100Hz. Because, in general, damping of the vibration in wide frequency region causes some degradation in performance. Low frequency limit is set because acceleration sensors in this vibration isolation system are insensitive in the frequency region lower than 0.1Hz. And high frequency limit is set because the ground motion is small enough in the frequency region higher than 100Hz. It is found in the huddling test that the vibration on the table with the active isolation control cannot be measured because the amplitude of the vibration is too small. So the damping factor in case of the active isolation control is only the limit value. Actual damping factor is speculated to be bigger than this value. Fig.8 shows the results of huddling test, in which all the sensors are placed together in a small area in the same direction and

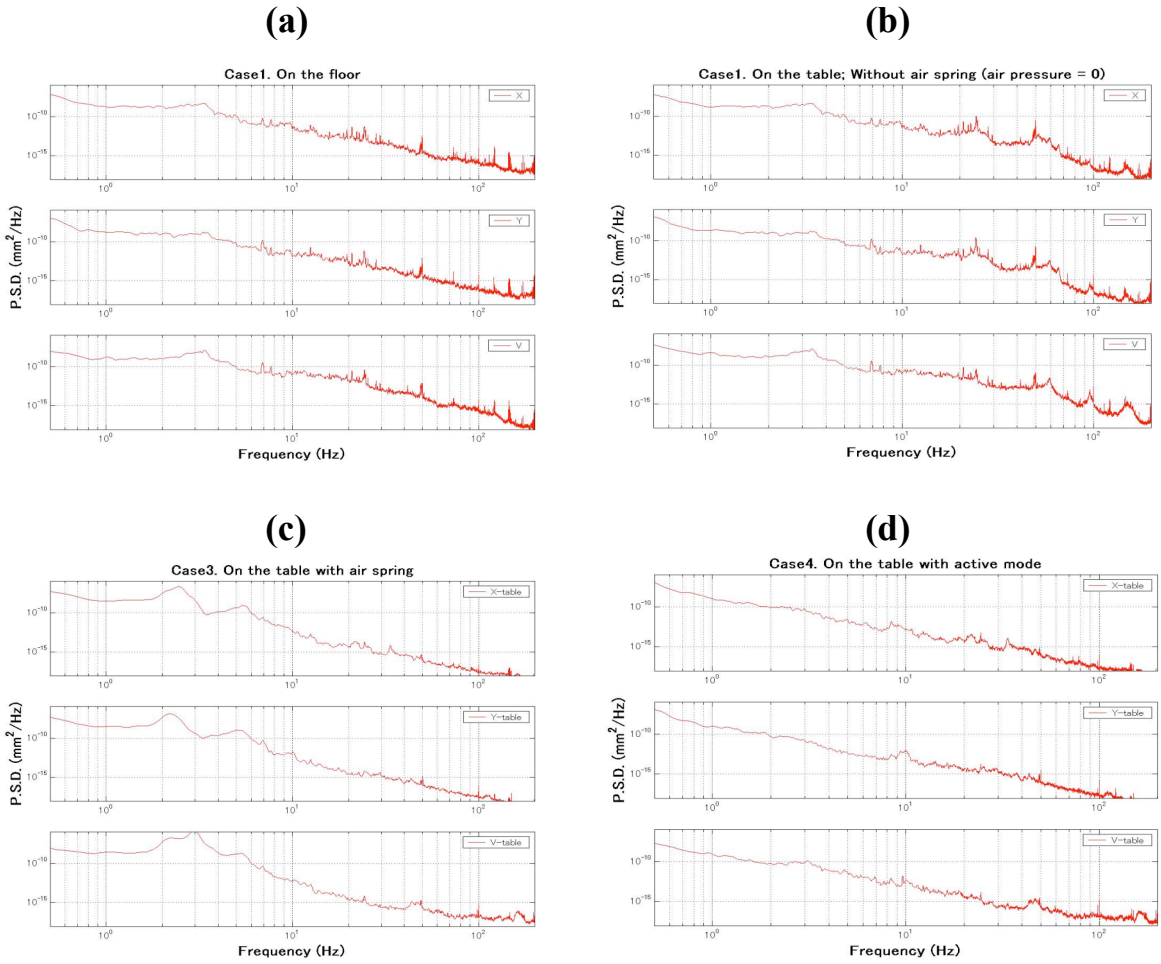

Fig. 6 PSD (Power Spectrum Density) for the vibration (a) on the floor, and those on the table (b) without air spring, (c) with air spring and (d) with active isolation. Top, middle and bottom figures in each row show PSD for the vibration in X, Y and Z directions.

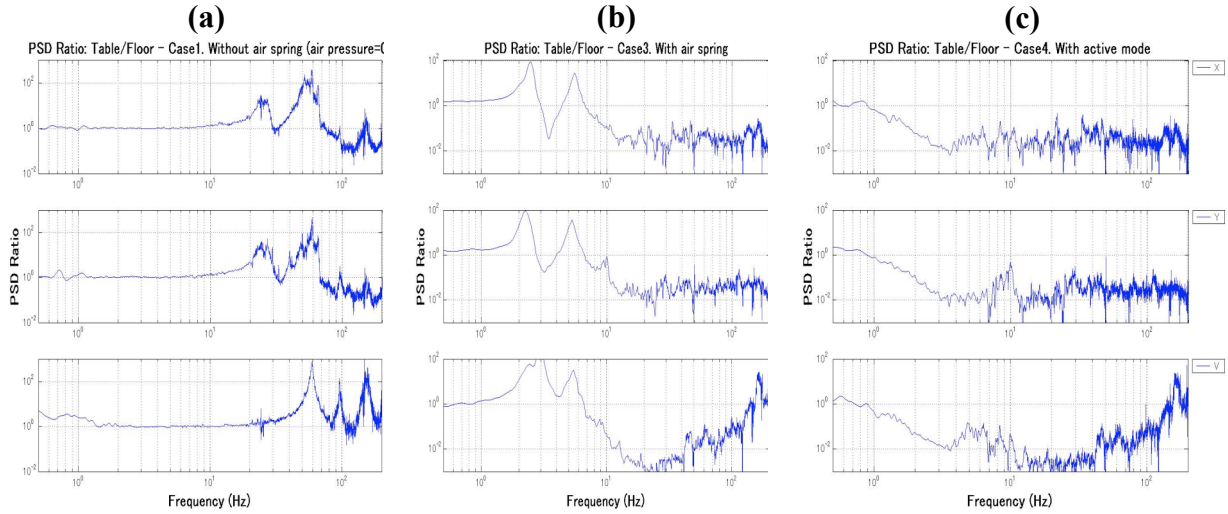

Fig. 7 PSD ratio of the vibration on the table to that on the floor; (a) without air spring, (b) with air spring and (c) with active isolation. Top, middle and bottom figures in each row show PSD ratio for the vibration in X, Y and Z directions.

coherence between sensors is checked. In each figure, the top graphs show the coherence for S1-S1, S1-S2 andS1-S3, and bottom ones show that for S3-S3, S3-S4 and S3-S6, where Si stands for the i-th sensor. Fig.8 (a) and (b) show coherence on the floor in X and Z direction, respectively. Fig.8 (c) and (d) show coherence on the table with active vibration isolation control for X and Z direction, respectively. These test results tell us that the vibration measurement is not good in the frequency region lower than 2Hz even on the floor, and the vibration on the table at active isolation control cannot be measured because the amplitude is too small.

5. SOUND NOISE

During the performance test, we sometimes experienced disturbance caused by sound. An announcement from a speaker, for example, shakes the table supported by the air spring. It

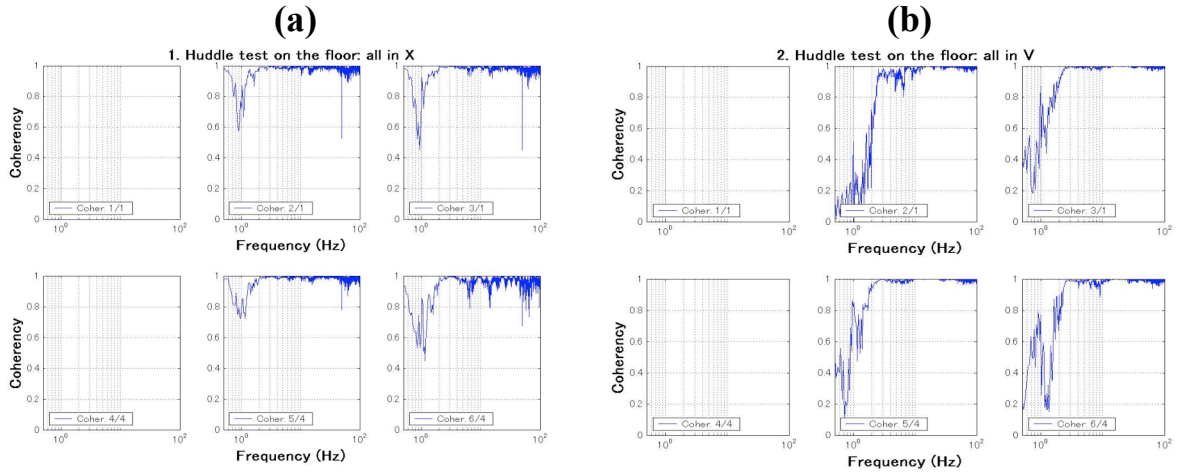

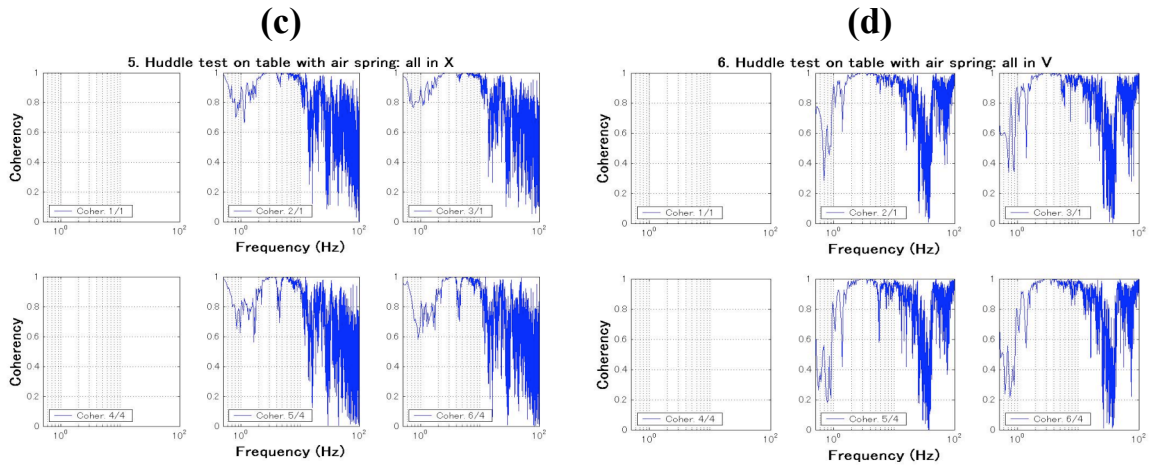

Fig. 8 Coherence in the huddling test of six sensors. (a) and (b) are results when all the sensors are placed on the floor in X and Z direction, respectively, and (c) and (d) are those when sensors are placed on the table in X and Z direction with active vibration isolation control, respectively. Top graphs in each figure show coherence for S1-S1, S1-S2 and S1-S3, and bottom graphs for S4-S4, S4-S5 and S4-S6, where Si stands for the i-th sensor.

occurs either in the passive mode or active mode. We looked for the resonance frequency by making sound with an electric oscillator and speakers. The floating table resonate most strongly with G# sound (208Hz) in horizontal direction. Results are shown in Fig.9. The time series plot for the signal from acceleration sensors, placed on the floor, is

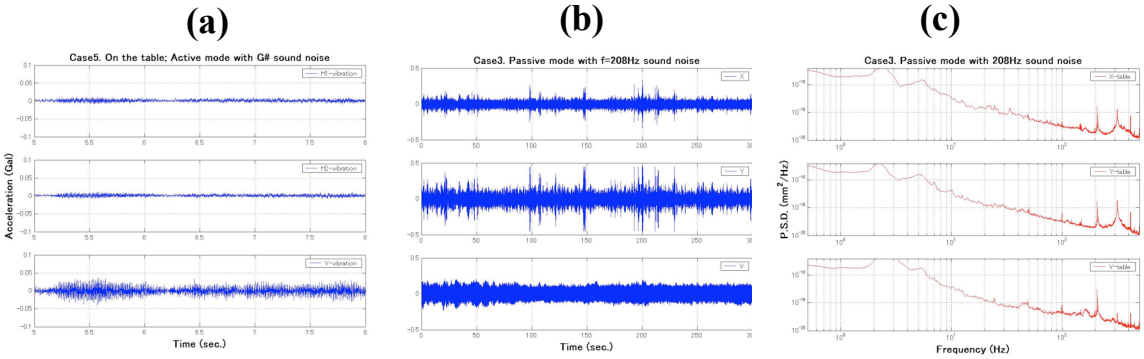

Fig. 9 (a) Time series plot for the signal from acceleration sensors placed on the floor. (b) Time series plot for the signal from sensors placed on the floating table supported with air spring, and (c) their PSD spectra. Top plot in each figure is that for X sensor, middle for Y and bottom for Z.

shown in Fig.9 (a) as a reference. Fig.9 (b) shows the time series plot for the signal from sensors placed on the table supported by the air spring, and (c) shows their PSD spectra, in which sharp peaks are seen at 200, 300 and 400Hz. Top, middle and bottom plots in each figure show those for X, Y and Z sensors, respectively. From these results, the shielding

against the sound noise will be important in actual use of the vibration isolation scheme to avoid eventual high frequency oscillation cause by sound noise.

6. SUMMARY

An active vibration isolation system was fabricated and its performance was tested. The vibration control is performed by eight pneumatic control valves installed at four pillars. The system has three acceleration sensors on the base, six acceleration sensors on the floating table and six displacement sensors to measure relative displacement between the base and table. Results of performance test are summarized in the following.

- Resonance structure is observed in the loop transfer function when a load of a skew-quadrupole magnet is placed on the table. This resonance structure is eliminated by installing a filter in the parameter-setting tables.

- Air pressure fluctuation causes the fluctuation of displacement. This position fluctuation can be reduced by raising displacement control gains. But these high gains degrade performance of acceleration feedback. We should reduce the air pressure fluctuation by installing high precision air regulators and keep low gains in the displacement control.

- Air spring (passive mode) damps high frequency vibration by two orders of magnitude in PSD in the frequency region higher than 10Hz. But it enhances low frequency peaks at 3 and 5Hz. Active vibration control (active mode) eliminates these low frequency peaks. We obtained limit value for the damping factor of one to two orders of magnitude in PSD in the frequency region 2 - 10Hz and two orders of magnitude in higher frequency region.

- We need seismometers having higher resolution to measure damping factor of vibration because the amplitude of vibration on the table at active mode is too small.

- Sound noise causes disturbance in the air spring support. Shielding against the sound noise will be important in actual use of the active vibration scheme.

References

[1] International Linear Collider Technical Review Committee Second Report, 2003, SLAC-R-606.
[2] H. Yoshioka and N. Murai, "An Active Microvibration Isolation System", Proceedings of 7th International Workshop on Accelerator Alignment, SPring-8, Harima, Japan, November 11-14, 2002.
[3] T. Mattison, "Vibration Control Feedback R&D at University of British Columbia", Contributed to the 26th Advanced ICFA Beam Dynamics Workshop on Nanometre-Size Colliding Beams, Lausanne, Switzerland, September 2-6, 2002.
[4] R. Assmann et. al., "CLIC Stability Study", Contributed to the 26th Advanced ICFA Beam Dynamics Workshop on Nanometre-Size Colliding Beams, Lausanne, Switzerland, September 2-6, 2002.